Pharmacology, Biochemistry and Behavior 100 (2011) 98–108

Contents lists available at ScienceDirect

Pharmacology, Biochemistry and Behavior

journal homepage: www.elsevier.com/locate/pharmbiochembeh

Extended access methamphetamine decreases immature neurons in the hippocampus which results from loss and altered development of neural progenitors without altered dynamics of the S-phase of the cell cycle

Clara J. Yuan [a], Jovy Marie D. Quiocho [b], Airee Kim [b], Sunmee Wee [b], Chitra D. Mandyam [a,b,*]

[a] Skaggs School of Pharmacy and Pharmaceutical Sciences, University of California San Diego, La Jolla, CA, USA
[b] Committee on the Neurobiology of Addictive Disorders, The Scripps Research Institute, La Jolla, CA, USA

ARTICLE INFO

Article history:
Received 13 May 2011
Received in revised form 13 July 2011
Accepted 5 August 2011
Available online 10 August 2011

Keywords:
Self-administration
Subgranular zone
Psychostimulant
BrdU
CldU
IdU
GFAP
Sox2
Ki-67
DCX
AC3

ABSTRACT

Methamphetamine addicts demonstrate impaired hippocampal-dependent cognitive function that could result from methamphetamine-induced maladaptive plasticity in the hippocampus. Reduced adult hippocampal neurogenesis observed in a rodent model of compulsive methamphetamine self-administration partially contributes to the maladaptive plasticity in the hippocampus. The potential mechanisms underlying methamphetamine-induced inhibition of hippocampal neurogenesis were identified in the present study. Key aspects of the cell cycle dynamics of hippocampal progenitors, including proliferation and neuronal development, were studied in rats that intravenously self-administered methamphetamine in a limited access (1 h/day: short access (ShA)-4 days and ShA-13 days) or extended access (6 h/day: long access (LgA)-4 days and LgA-13 days) paradigm. Immunohistochemical analysis of Ki-67 cells with 5-chloro-2′-deoxyuridine (CldU) demonstrated that LgA methamphetamine inhibited hippocampal proliferation by decreasing the proliferating pool of progenitors that are in the synthesis (S)-phase of the cell cycle. Double S-phase labeling with CldU and 5-iodo-2′-deoxyuridine (IdU) revealed that reduced S-phase cells were not due to alterations in the length of the S-phase. Further systematic analysis of Ki-67 cells with GFAP, Sox2, and DCX revealed that LgA methamphetamine-induced inhibition of hippocampal neurogenesis was attributable to impairment in the development of neuronal progenitors from preneuronal progenitors to immature neurons. Methamphetamine concomitantly increased hippocampal apoptosis, changes that were evident during the earlier days of self-administration. These findings demonstrate that methamphetamine self-administration initiates allostatic changes in adult neuroplasticity maintained by the hippocampus, including increased apoptosis, and altered dynamics of hippocampal neural progenitors. These data suggest that altered hippocampal plasticity by methamphetamine could partially contribute to methamphetamine-induced impairments in hippocampal function.

1. Introduction

Methamphetamine addiction presents significant social, economic, and public health problems worldwide. The United Nations Office on Drugs and Crime estimated that between 16 and 51 million people aged 15–64 years used amphetamines at least once in 2007 (UNODC, 2009). Clinical studies in humans who were under the influence of moderate to heavy methamphetamine use demonstrated a variety of hippocampal-dependent cognitive deficits that can persist for days after abuse and cannot be recovered during abstinence (Roehr, 2005; Schwartz et al., 2010; Simon et al., 2010), as well as a considerable incidence of relapse (Newton et al., 2009). Therefore, it appears that several neuroadaptations in the hippocampus can occur after methamphetamine abuse that could contribute to the memory deficits, rewarding effects, and relapse behaviors associated with the drug (Rogers et al., 2008; Thompson et al., 2004).

Recent research revealed that the hippocampus is an important site of adult neurogenesis—the process of birth, survival, and integration of granule cell neurons in the dentate gyrus of the adult hippocampus (Altman and Das, 1965). Notably, maturation of hippocampal progenitors into glutamatergic neurons in adulthood is thought to contribute to and maintain adult hippocampal structure and function (Earnheart et al., 2007; Ge et al., 2007; Gould et al., 1999; Hastings et al., 2001; Kaplan and Hinds, 1977; Shors et al., 2002; Tashiro et al., 2007). For example, procedures, such as low doses of irradiation, have been used to ablate the birth of proliferating progenitors in the hippocampal dentate gyrus, and changes in the animal's environment (e.g., voluntary wheel running in the home cage) have been used to enhance the proliferation and maturation of

* Corresponding author at: Committee on the Neurobiology of Addictive Disorders, The Scripps Research Institute, 10550 North Torrey Pines Road, SP30-2400, La Jolla, CA 92037, USA. Tel.: +1 858 784 9039; fax: +1 858 784 2086.
E-mail address: cmandyam@scripps.edu (C.D. Mandyam).

0091-3057/$ – see front matter © 2011 Elsevier Inc. All rights reserved.
doi:10.1016/j.pbb.2011.08.004

hippocampal progenitors to provide a functional link between hippocampal neurogenesis and hippocampal-dependent memory (Madsen et al., 2003; Raber et al., 2004; Rola et al., 2004; van Praag et al., 1999a, 1999b). With respect to hippocampal neurogenesis and drug addiction, various correlative studies have demonstrated that drug of abuse-induced reductions in adult neurogenesis may contribute to drug-induced maladaptive plasticity in the hippocampus (Brown et al., 2010; Eisch and Harburg, 2006; Noonan et al., 2008; Sudai et al., 2011). Furthermore, neurogenesis and non-neurogenesis studies have used similar mechanistic approaches as those used for hippocampal memory studies (i.e., irradiation and wheel running) to demonstrate a functional role for adult-generated hippocampal neurons in drug taking and drug seeking (Cosgrove et al., 2002; Noonan et al., 2010; Smith et al., 2008; Smith et al., 2011; Thanos et al., 2010). Therefore, evidence shows that adult hippocampal neurogenesis can play a role in manipulating behaviors that underlie the addiction process. However, more evidence is required to demonstrate that the dysregulation in the process of generation and maintenance of adult-generated hippocampal neurons could increase the vulnerability to drug addiction (Canales, 2007, 2010).

Recent evidence has shown that some aspects of hippocampal neurogenesis could be involved in the altered neuroplasticity that underlies methamphetamine addiction. Experimenter-delivered (Hildebrandt et al., 1999; Kochman et al., 2009; Teuchert-Noodt et al., 2000) and clinically relevant models of intravenous self-administration (Mandyam et al., 2008b) of methamphetamine in rodents negatively impact the proliferation and survival of adult hippocampal neural progenitors. Experimenter-delivered and self-administered methamphetamine produces hippocampal cell death (Mandyam et al., 2008b; Schmued and Bowyer, 1997), suggesting a potential role for hippocampal cell death in methamphetamine addiction. Thus, while there is preliminary evidence supporting the devastating effects of methamphetamine on adult hippocampal neuroplasticity, little information exists on the mechanisms underlying these effects.

Some important advances have been made to determine the mechanisms underlying methamphetamine-induced inhibition of hippocampal neurogenesis. Experimenter-delivered methamphetamine decreased 7-day-old 5-bromo-2′-deoxyuridine cells (BrdU; single injection of BrdU labels S-phase cells, and the age of the cell at the time of euthanasia determines proliferation, differentiation, and maturation stages; (Eisch and Mandyam, 2007)), suggesting that methamphetamine inhibited the proliferation or maturation of neural progenitors (Hildebrandt et al., 1999; Teuchert-Noodt et al., 2000). Self-administration of methamphetamine (42 days of limited and extended access to methamphetamine) decreased Ki-67-labeled proliferating cells (Ki-67 is expressed in proliferating hippocampal progenitors in S, G_2, M, and parts of G_1 phases of the cell cycle (Gerdes et al., 1984)), and immature doublecortin (DCX) neurons indicating that methamphetamine inhibits the proliferation and maturation of neural progenitors (Mandyam et al., 2008b). Detailed phenotype analysis of DCX cells in the self-administration study revealed that DCX cells that expressed Ki-67 (i.e., early neuronal cells, type2b/3) were significantly decreased by methamphetamine, demonstrating a mechanism for methamphetamine-induced inhibition of neurogenesis (Mandyam et al., 2008b). However, it needs to be determined whether methamphetamine-induced inhibition of Ki-67 cells occurs at a time frame earlier than 42 days of methamphetamine self-administration and whether a reduction in Ki-67 cells results from a reduced pool of neural progenitors in distinct phases of the cell cycle (e.g., S-phase of the cell cycle) and alterations in the dynamics of the S-phase. Given that hippocampal neurogenesis is now appreciated as a multi-stage process (Steiner et al., 2006), and specific stages of neurogenesis are differentially regulated by antidepressants, wheel running, opiates and alcohol (Arguello et al., 2008; Encinas et al., 2006; Kronenberg et al., 2003; Taffe et al., 2010), it is unclear how the distinct stages of neurogenesis are affected by methamphetamine. Furthermore, since non-neurogenesis studies demonstrate that cell death occurs immediately following a single day of methamphetamine exposure (Morgan and Gibb, 1980; Schmued and Bowyer, 1997), and hippocampal cell death may contribute to decreases in SGZ proliferation, additional earlier time points of methamphetamine self-administration should be examined for changes in proliferation and cell death. Therefore, in this study, we sought to describe the mechanisms by which methamphetamine reduces the proliferation of neural progenitors by identifying certain aspects of proliferation and the distinct stages of neuronal development.

2. Materials and methods

2.1. Animals and tissue preparation

Adult, male Wistar rats (Charles River), weighing 200–250 g at the start of the experiment, were housed two per cage in a temperature-controlled vivarium under a reverse light/dark cycle (lights off 10:00 a.m.–10:00 p.m.). Food and water were available ad libitum. Animals underwent surgery for catheter implantation for intravenous methamphetamine self-administration (Mandyam et al., 2007). For baseline training sessions, the animals were allowed to self-administer methamphetamine at a dose of 0.05 mg/kg/injection under a fixed-ratio 1 (FR1) schedule for seven sessions (baseline sessions). After baseline training, the rats were divided into four groups balanced by the number of injections per session during the last three baseline sessions. During the escalation period, two groups of rats (long-access; LgA-4 days (d), LgA-13 d; $n=7$ per group) were allowed to self-administer 0.05 mg/kg/injection of methamphetamine for 6 h per day under an FR1 schedule, whereas the other groups (short-access; ShA-4 d, ShA-13 d; $n=7$ per group) were allowed to do so for 1 h per day under an FR1 schedule. A complete description of the methamphetamine self-administration protocol is provided in (Mandyam et al., 2008b). All procedures were performed during the dark cycle. On day 5, (16–22 h after the last methamphetamine intake), ShA-4 d and LgA-4 d rats received one injection of 50 mg/kg 5-chloro-2′-deoxyuridine (CldU, i.p.; Sigma, cat# C6891; dissolved in 0.9% saline and 0.007 N NaOH at 5 mg/ml) and survived for 30 min. On day 14, (14–20 h after the last methamphetamine intake), ShA-13 d and LgA-13 d received one injection of 50 mg/kg 5-Iodo-2′-deoxyuridine (IdU; MP Biomedicals, cat# 100357; dissolved in 0.9% saline, 0.2 N NaOH at 2.5 mg/ml, normalized to pH 7 with 10 N HCl) followed by 50 mg/kg CldU 2 h later. These rats also survived for 30 min after the CldU injection. A parallel group of drug-naive rats ($n=6$) received one injection of 50 mg/kg IdU followed by 50 mg/kg CldU 2 h later. These rats also survived for 30 min after the CldU injection. A separate group of drug-naive rats was injected with IdU ($n=2$), CldU ($n=2$), or BrdU ($n=3$; all 50 mg/kg) separately and survived for 2 h after the injection. All animals were 12–13 weeks old when anesthetized with chloral hydrate and perfused transcardially as described previously (Mandyam et al., 2008b). Serial coronal 40 μm sections were obtained on a freezing microtome, and sections from the hippocampus (bregma −1.4 to −6.7; Paxinos and Watson, 1997) were stored in 0.1% NaN_3 in 1X phosphate-buffered saline (PBS) at 4 °C. Surgical and experimental procedures were carried out in strict adherence to the *National Institutes of Health Guide for the Care and Use of Laboratory Animals* (NIH publication number 85–23, revised 1996) and approved by the Institutional Animal Care and Use Committee of The Scripps Research Institute.

2.2. Antibodies

The following primary antibodies were used for immunohistochemistry: chicken polyclonal anti-glial fibrillary acidic protein

(GFAP; 1:500; Abcam), rabbit monoclonal anti-Ki-67 (1:1000; Novocastra), mouse monoclonal anti-BrdU (1:10, Abcam; 1:100–1:500, BD Biosciences), rat monoclonal anti-BrdU (1:400; Serotec), goat polyclonal anti-doublecortin (DCX; 1:700; Santa Cruz Biotechnology), goat polyclonal anti-sex-determining region Y-box 2 (Sox2; 1:50; Santa Cruz Biotechnology), and rabbit polyclonal anti-activated caspase 3 (AC-3; 1:500; Cell Signaling).

2.3. Immunohistochemistry

The left and right hemispheres through the rat brain hippocampus were slide-mounted, coded, and dried overnight prior to immunohistochemistry. Sections were pretreated (Mandyam et al., 2004), blocked, and incubated with the primary antibodies, followed by fluorescent (for Ki-67, CldU, and IdU) or biotin-tagged (for DCX and AC-3) secondary antibodies.

2.3.1. Microscopic analysis and quantification

For fluorescent Ki-67, CldU, IdU, bright-field DCX, and AC-3 analyses, SGZ cells (i.e., cells touching and within three cell widths inside and outside the hippocampal granule cell-hilus border) were quantified with a Zeiss Axiophot photomicroscope (400× magnification) using the optical fractionator method in which sections through the hippocampus (bregma −1.4 to −6.7) were examined (Paxinos and Watson, 1997).

2.3.2. Proliferating cells in S-phase

Fluorescent labeling of every eighteenth section through the hippocampus was used for analysis. Sections from rats in the control, ShA-4 d, ShA-13 d, LgA-4 d, and LgA-13 d groups were double-labeled with antibodies for Ki-67 and CldU, and the number of cells that were Ki-67 alone, CldU alone or CldU/Ki-67 was quantified.

2.3.3. S-phase analyses

A pilot study was conducted first to test the specificity of antibodies that have been used to detect the thymidine analogs BrdU, IdU, and CldU (Leuner et al., 2009) in animals that received only one of these markers at a dose of 50 mg/kg. The specific labeling of each marker with commercially available antibody was determined by fluorescent labeling (Fig. 3a–f). We used two antibodies to detect IdU cells, namely, mouse monoclonal anti-BrdU from BD Biosciences (1:100 to 1:500; cat# 347580) and mouse monoclonal anti-BrdU from Abcam (1:10; cat# ab8152). The BD antibody labeled cells in brain tissue from IdU-only and CldU-only injected rats at all dilutions tested (could not detect either IdU or CldU beyond 1:500 dilution). Therefore, BD antibody did not show specificity to IdU, supporting a recent study that reported a similar pattern of staining with higher concentrations of the markers (Leuner et al., 2009). The Abcam antibody at the dilution used (1:10) did not show any labeling in the brain tissue from CldU only-injected rats and showed a similar labeling pattern compared with the BD antibody in the brain tissue from IdU only-injected rats. Next, at the dilution tested, the rat monoclonal anti-BrdU from Serotec (1:400; cat# MCA2060) showed specific labeling in brain tissue from CldU only-injected rats. No labeling was seen in brain tissue from IdU only-injected rats (Fig. 3a–f). All antibodies showed specific staining in brain tissue from BrdU only-injected rats (data not shown). Lastly, the fluorescently labeled BrdU, CldU, and IdU cells in every ninth section through the hippocampus were quantified using the optical fractionator method on hippocampal tissue to quantify and compare the labeling of IdU, CldU, and BrdU cells.

2.3.4. Length of S-phase

After confirming the 50 mg/kg dose to be equi-effective (i.e., labeled equal number of BrdU, IdU, and CldU cells), fluorescent double-labeling of CldU/IdU was performed for S-phase analysis. To determine the *S*-phase of the cell cycle, proliferating cells in the *S*-

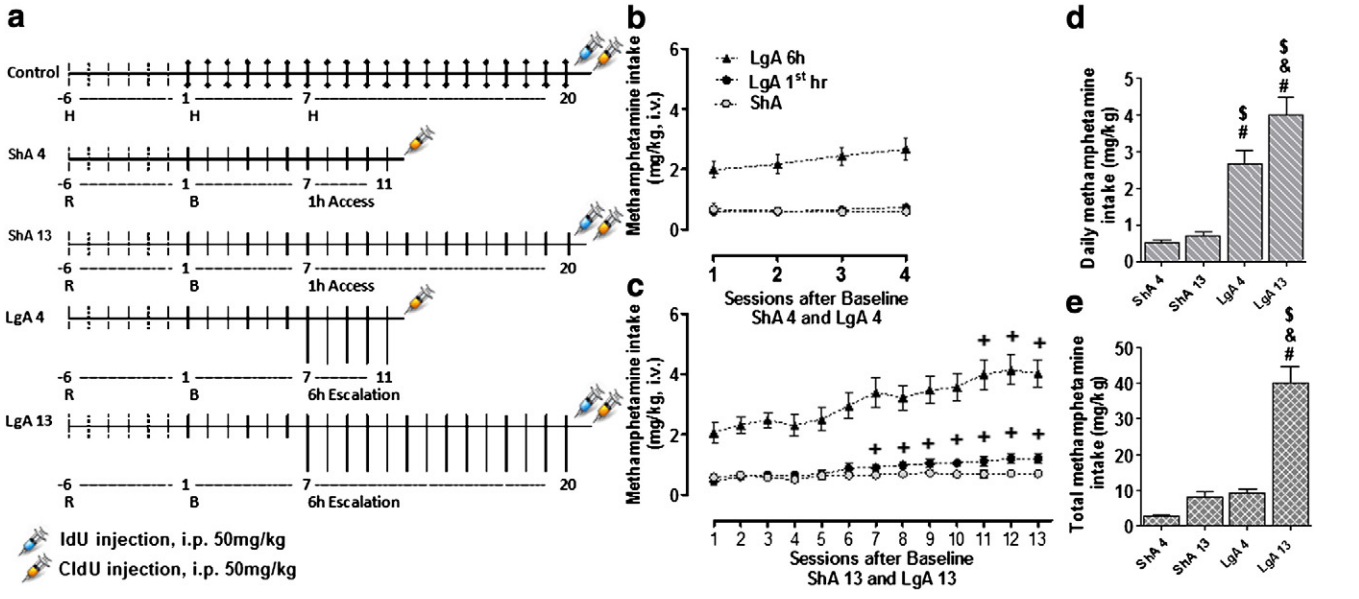

Fig. 1. Timeline of methamphetamine self-administration and injection of mitotic markers: daily and total methamphetamine intake. (a) Schematic of the timeline of methamphetamine self-administration: control (drug-naive), short access for 4 days (ShA-4 d), short access for 13 days (ShA-13 d), long access for 4 days (LgA-4 d), and long access for 13 days (LgA-13 d). Each vertical line in (a) represents 1 day, with the length corresponding to the duration of access. Closed lines in the control indicate that animals were not given access to drug and were only handled each day. H, handled; R, recovery from surgery; B, baseline training for methamphetamine acquisition; yellow needles, chlorodeoxyuridine (CldU) injection; blue needles, iododeoxyuridine (IdU) injection. (b) Methamphetamine intake (mg/kg) over time after baseline in ShA-4 d and LgA-4 d animals. Gray circles, ShA-4 d; black circles, 1st-hour access of LgA-4 d; black triangles, LgA-4 d. (c) Methamphetamine intake (mg/kg) over time after baseline in ShA-13 d and LgA-13 d animals. Gray circles, ShA-13 d; black circles, 1st-hour access of LgA-13 d; black triangles, LgA-13 d. $^{+}p<0.05$, significantly different from 1st-day access. Daily and total methamphetamine intake (mg/kg) are shown in (d) and (e), respectively, for ShA-4 d, ShA-13 d, LgA-4 d, and LgA-13 d. $^{\&}p<0.05$, compared with LgA-4 d; $^{\#}p<0.05$, compared with ShA-4 d; $^{\$}p<0.05$, compared with ShA-13 d.

phase were pulse-chased with low doses of exogenous markers IdU and CldU (50 mg/kg each, i.p.; Breunig et al., 2007; Burns and Kuan, 2005; Maslov et al., 2004; Vega and Peterson, 2005), and the length of the *S*-phase was calculated using the parameters according to Cameron and McKay (Cameron and McKay, 2001) and Hayes and Nowakowski (Hayes and Nowakowski, 2002). IdU and CldU (Figs. 1a and 3a) were used sequentially to label *S*-phase cells at two time-points ($T_1 = 0$ h, $T_2 = 2$ h, a time-point less than the G_2/M-phase; Cameron and McKay, 2001). Control, ShA-13 d, and Lga-13 d rats were given one injection of IdU followed by CldU 2 h (T_2) later on day 14 after the methamphetamine sessions. Every eighteenth section through the hippocampus was used for analysis. Fluorescently labeled brain tissue from animals sequentially injected with IdU and CldU (CY2 for IdU and CY3 for CldU, respectively; Fig. 3c–e) revealed three distinct populations of proliferating cells in the *S*-phase, some cells labeled with rat antibody only, some labeled with mouse antibody only, and most colabeled with both antibodies (Fig. 3f). The labeling pattern was quantified as the following: single-labeled IdU (number of cells that exit the *S*-phase during $T_2 = 2$ h, N_{EX}), single-labeled CldU (number of cells that enter the *S*-phase during $T_{CldU} = 30$ min, N_{EN}), and double-labeled IdU/CldU cells. Based on previous reports, the expected value (E) of the proportion of dividing cells in the *S*-phase at any given time point was equal to the proportion of cell cycle time of the *S*-phase labeled with a single *S*-phase marker (Cameron and McKay, 2001; Hayes and Nowakowski, 2000; Nowakowski et al., 1989). The calculation of the length of the *S*-phase (T_S) was performed as the following:

$$\text{Therefore, } E\left\{\frac{N_{EX}}{N_S}\right\} = \frac{T_{EX}}{T_S}$$

$T_{EX} = T_2 =$ interinterval time (2 h; Fig. 3a)

Total number of cells labeled with mouse BrdU antibody (IdU) $= N_{IdU}$

Total number of cells labeled with rat BrdU antibody = CldU cells = cells in $S-$phase $N_S = N_{CldU}$

Cells that exited the $S-$phase and entered the $G_2/M-$phase at T_2 $= \left(N_{IdU\ single}\right) = N_{EX}$

Time $-$line of $S-$phase $T_S = T_2/(N_{EX}/N_C)$

T_S values were calculated individually for each rat.

2.3.5. Confocal microscopy

Confocal analysis was performed on individual CldU-immunoreactive (IR), IdU-IR, and Ki-67-IR cells at 600× magnification. Optical sectioning in the *z*-plane was performed using multitrack scanning with a section thickness of 0.45 μm. Colocalization of antibodies was assessed with the confocal system by analysis of adjacent *z*-sections (gallery function and orthogonal function for equal penetration of the antibodies). For the proportion of Ki-67 cells in the *S*-phase study, cells that were Ki-67 alone or CldU alone were quantified and multiplied by 18 to give the total number of cells, and the proportion of Ki-67 cells that were $CldU^+$ was also calculated. For the *S*-phase study, the number of cells that were IdU alone, CldU alone, and IdU/CldU labeled were quantified and are shown as raw data for each animal.

2.3.6. Phenotype of Ki-67 cells

Fluorescent labeling of every twenty seventh section through the hippocampus was used, and qualitative analyses were performed as reported previously (Taffe et al., 2010). Two sets of triple-labeling were performed: Set 1 with Ki-67/GFAP/Sox2 and Set 2 with Ki-67/Sox2/DCX. Ki-67 cells were marked in distinct stages of neuronal development: radial glia-like stem cells (type1), pre-neuronal neuroblasts (type2a), intermediate cells (type2b), and immature neurons (type3) based on original descriptions (Steiner et al., 2006). Type1 cells were labeled as $GFAP^+/Sox2^+/Ki\text{-}67^+$. Type2a cells were labeled as $Sox2^+/Ki\text{-}67^+/DCX^-$. Type2b cells were labeled as $Sox2^+/Ki\text{-}67^+/DCX^+$. Type3 cells were labeled as $Sox2^-/Ki\text{-}67^+/DCX^+$ cells. Confocal analysis was performed on individual Ki-67-IR cells at 600× magnification for both sets of triple-labeling. Colocalization of antibodies was assessed with the confocal system by analysis of adjacent *z*-sections (gallery function and orthogonal function for equal penetration of the antibodies). The percentage of Ki-67-IR cells that were $GFAP^+/Sox2^+$, $Sox2^+/DCX^+$, or Sox2-/DCX^+ in relation to the total number of Ki-67 cells was analyzed for each rat as follows: Set 1 triple-labeling produced data for $Ki\text{-}67^+/GFAP^+/Sox2^+$ cells; Set 2 triple-labeling produced data for $Ki\text{-}67^+/Sox2^+/DCX^-$, $Ki\text{-}67^+/Sox2^+/DCX^+$, and $Ki\text{-}67^+/Sox2^-/DCX^+$ cells. The proportion of Ki-67 cells that were not labeled for Sox2 and DCX were analyzed from Set 2 triple-labeling as Ki-67 and GFAP, always stained with Sox2, and never seen as Ki-67/GFAP-alone cells in our labeling.

2.3.7. Immature neurons/neurogenesis

For brightfield DCX analysis, morphological details were examined from every ninth section through the hippocampus that was stained by the DAB method to mark the differentiating/maturing cells. Specifically, early-phase (immature type) DCX-IR cells were separately analyzed from late-phase (mature type) DCX-IR cells, with early-phase cells having short processes and late-phase cells having long processes that extend into the molecular layer of the dentate gyrus (Fig. 5a; Mandyam et al., 2008a, 2008b).

2.3.8. Cell death/apoptosis

Cell death analysis was performed on every ninth section through the hippocampus with a marker for activated caspase-3 that labels apoptotic cells. AC3-labeled cells in the SGZ and granule cell layer were counted. All microscopic quantifications and analyses were performed by an observer blind to the study.

2.4. Data analysis

The methamphetamine self-administration data are expressed as the mean mg/kg per session of methamphetamine self-administration for each group of rats. The effect of session duration on methamphetamine self-administration per session as well as in the first hour of a session was examined over the 13 escalation sessions using a two-way repeated-measures analysis of variance (ANOVA; session duration × daily session; SPSS software) followed by Fisher's Least Significant Difference (LSD) post hoc test. The pattern of responding for methamphetamine is expressed as the mean mg/kg per hour over 6 h sessions in LgA rats and compared between the first and 13th escalation sessions. Differences in the rate of responding between the first and other escalation sessions were evaluated using the paired *t*-test (Prism 5.0, GraphPad, San Diego, CA). Methamphetamine self-administration, CldU, Ki-67, DCX, and activated AC3 data were analyzed using one-way or two-way ANOVA, with methamphetamine access and the technical aspects of cell markers as variables using SPSS software. The analysis of phenotypes was also done using non-matching two-way ANOVA, with methamphetamine access and Ki-67 or CldU cell phenotype as variables. All analyses were followed by Fisher's LSD post hoc test. Data are expressed as mean ± SEM. Values of $p < 0.05$ were considered statistically significant. Graphs were generated using GraphPad Prism 5.0 software. Images presented here were collected on a confocal microscope (LaserSharp 2000, version 5.2, emission wavelengths 488, 568, and 647 nm; Bio-Rad Laboratories) and imported into Photoshop (version CS2). Only the gamma adjustment in the Levels function was used.

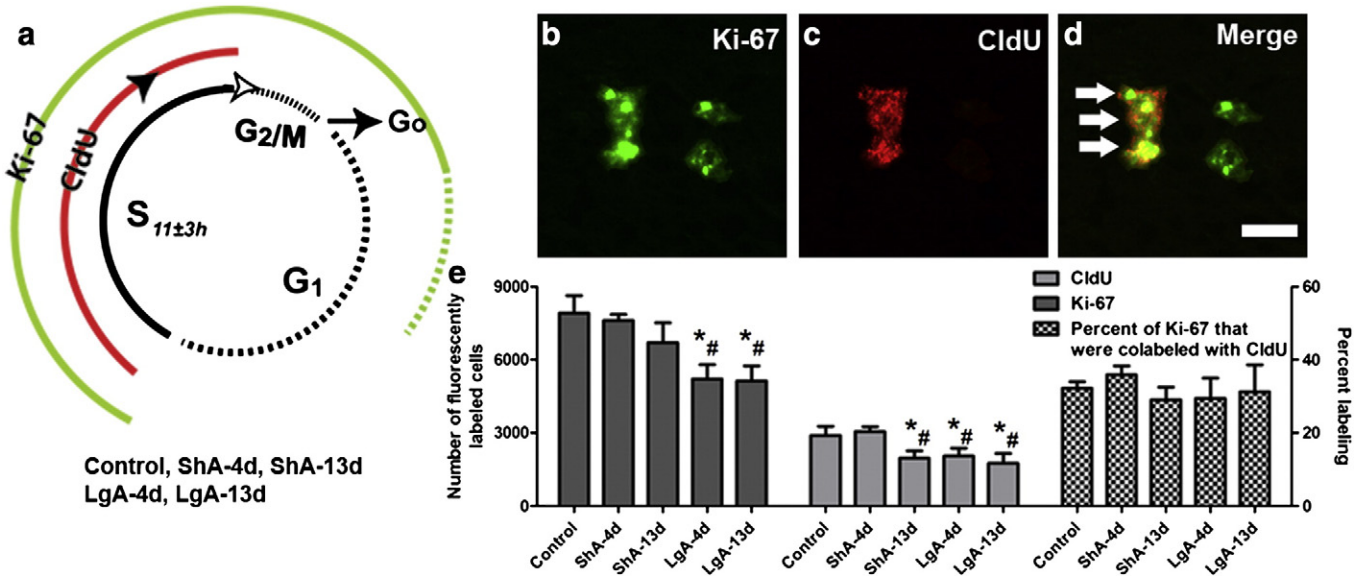

Fig. 2. Methamphetamine self-administration decreases proliferation of hippocampal progenitors and specifically decreases cells in the *S*-phase of the cell cycle. Hippocampal sections from all groups were co-labeled with CldU and Ki-67, and the number of Ki-67 and CldU cells was quantified. (a) Schematic representation of labeling pattern for Ki-67 and CldU during different phases of the cell cycle of adult rat progenitor cells. The length of the *S*-phase of the cell cycle is estimated to be 11 ± 3 h. (b–d) Single *z*-scan (0.5 mm) of a confocal *z*-stack of Ki-67-IR in green (FITC) and CldU + cells in red (CY3). Arrows in (d) point to double-labeled cells. Scale bar in (d) = 10 μm and applies to (b–d). (e) Quantitative analysis of fluorescently labeled Ki-67 and CldU cells from each group of rats (left Y-axis). The proportion of Ki-67 cells that were labeled with CldU is also indicated (right Y-axis). Data are expressed as mean ± SEM. $^{*}p<0.05$, compared with control; $^{\#}p<0.05$, compared with ShA-4 d.

3. Results

3.1. Extended access to methamphetamine produces escalation in methamphetamine intake in animals that self-administered for 13 days

Methamphetamine self-administration in a LgA paradigm occurred for either 4 days (a time-point prior to escalation in methamphetamine intake) or 13 days (a time-point post-escalation in methamphetamine intake; Fig. 1a; Kitamura et al., 2006; Mandyam et al., 2007). Methamphetamine self-administration in a ShA paradigm was run in parallel. A total of four groups were included: ShA-4 d, ShA-13 d, LgA-4 d, and LgA-13 d. Escalation in methamphetamine intake was not evident in the ShA-4 d and ShA-13 d groups and LgA-4 d group (Fig. 1b, c). Methamphetamine intake, when expressed as daily intake ($F_{3,28}=32.2$, $p<0.001$) or total intake ($F_{3,28}=48.5$, $p<0.001$), was significantly different between groups (Fig. 1d, e). Post hoc analyses indicated that daily methamphetamine intake in the LgA-13 d group differed from the ShA-4 d, ShA-13 d, and LgA-4 d groups ($p<0.001$). Daily methamphetamine intake in the LgA-4 d group differed from the ShA-4 d and ShA-13 d groups ($p<0.01$). The ShA-4 d and ShA-13 d groups did not differ from each other. Total methamphetamine intake in the LgA-13 d group differed from the ShA-4 d, ShA-13 d, and LgA-4 d groups ($p<0.001$). The ShA-4 d, ShA-13 d, and LgA-4 d groups did not differ from each other. Methamphetamine self-administration in LgA-13 d animals during the first hour was considerably higher in sessions 7–13 vs. the first session and during the total 6 h was higher in sessions 11–13 vs. the first sessions ($p<0.05$; Fig. 1c).

3.2. Four days and 13 days of extended but not limited access to methamphetamine self-administration decreases Ki-67 cells; reduced Ki-67 cells are attributable to fewer proliferating cells in the S-phase of the cell cycle

Hippocampal progenitors that were in all phases of the cell cycle were labeled with Ki-67, an endogenous marker of proliferation. Hippocampal progenitors that were in the S-phase of the cell cycle were labeled with CldU (CldU is a marker that labels only *S*-phase cells at the 30 min survival time point), an exogenous marker of proliferation (Fig. 2a). Fluorescently labeled Ki-67^{+} cells and CldU^{+} cells were quantified from the same sections (Fig. 2b–d). Methamphetamine significantly decreased the number of Ki-67 cells ($F_{4,34}=3.7$, $p=0.02$; Fig. 2e, Ki-67). Post hoc analysis indicated that the LgA-4 d ($p=0.013$) and LgA-13 d ($p=0.025$) groups had significantly fewer Ki-67^{+} cells than controls. Methamphetamine self-administration decreased the number of CldU cells ($F_{4,34}=3.5$, $p=0.025$; Fig. 2e, CldU). Post hoc analyses indicated that controls were significantly different from ShA-13 d ($p=0.054$), LgA-4 d ($p=0.051$), and LgA-13 d ($p=0.047$) animals. The ShA-4 d group was significantly different from the ShA-13 d group ($p=0.02$) and LgA-4 d and LgA-13 d groups ($p=0.01$). Lastly, the proportion of Ki-67 cells that were co-labeled with CldU was determined in the same

Fig. 3. (a–i) Antibodies generated for bromodeoxyuridine distinctly label IdU- and CldU-immunoreactive cells. Technical information about the antibodies used is provided in the figure. (a–c) Animals injected with IdU only do not show any immunolabeling with the rat anti-BrdU antibody, and (d–f) animals injected with CldU only do not show any immunolabeling with mouse anti-BrdU. Staining is shown in the subventricular zone of adult rats that received one injection of IdU (a–c), one injection of CldU (d–f), or IdU and CldU (g–i) 30 min before euthanasia. The thin arrows in (a–i) point to IdU only-positive cells. The thick arrows in (a–i) point to CldU-only cells. The arrowheads in (g–i) point to double-labeled IdU/CldU cells. (j) Schematic of the cell cycle of adult rat SGZ progenitors, including the phases during which CldU and IdU cells are labeled. Control, ShA-13 d, and LgA-13 d animals were injected with 50 mg/kg Idu at T_1 and injected with 50 mg/kg CldU 2 h (T_2) later. Sections from these animals were then labeled with antibodies for BrdU, and the number of cells that were IdU alone, CldU alone, and IdU/CldU was quantified. The timeline of the *S*-phase is 11 ± 3 h. (k–m) Single *z*-scan (0.5 mm) of a confocal *z*-stack of CldU^{+} cells in red (CY3) and IdU + cells in green (CY2). The thick arrow in (m) points to a double-labeled IdU/CldU cell. Scale bar in (m) = 10 μm and applies to (k–m). (n) Methamphetamine self-administration does not alter the length of the *S*-phase. Number of IdU (N_{EX}), CldU (N_{EN}), and IdU/CldU (N_S) cells represented as raw data per animal (left Y-axis). The length of the *S*-phase (T_S in hours) calculated from the raw data (see Methods) for control, ShA-13, and LgA-13 (right Y-axis). Data are expressed as mean ± SEM. $^{*}p<0.05$, compared with control. CldU^{+}/IdU^{+} cells and CldU^{+}/Ki-67^{+} cells.

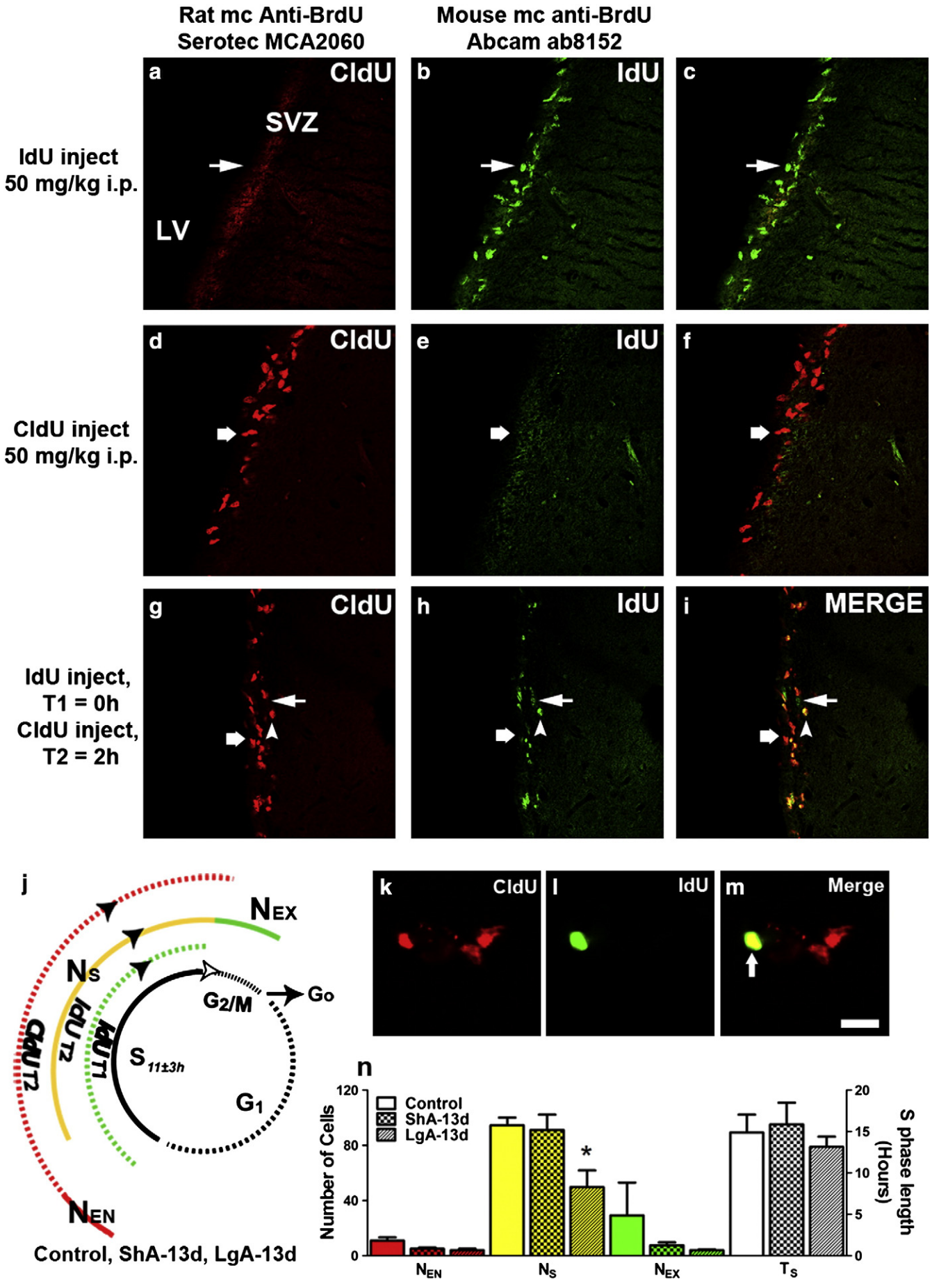
Rat mc Anti-BrdU
Serotec MCA2060
Mouse mc anti-BrdU
Abcam ab8152
IdU inject
50 mg/kg i.p.
CldU inject
50 mg/kg i.p.
IdU inject,
T1 = 0h
CldU inject,
T2 = 2h
a
CldU
SVZ
LV
b
IdU
c
d
CldU
e
IdU
f
g
CldU
h
IdU
i
MERGE
j
NEX
NS
G2/M
Go
S11±3h
G1
NEN
Control, ShA-13d, LgA-13d
k
CldU
l
IdU
m
Merge
n
Control
ShA-13d
LgA-13d
Number of Cells
S phase length (Hours)
NEN
NS
NEX
TS

sections. Methamphetamine did not alter the proportion of Ki-67 cells that were $CldU^+$ (Fig. 2e, Ki-67/CldU).

3.3. IdU and CldU produce equivalent labeling of hippocampal progenitors compared with BrdU at lower doses

Drug-naive animals were injected with one of the mitotic markers IdU, CldU, or BrdU at a concentration of 50 mg/kg and survived for 2 h post injection. Another group of drug-naive animals were injected with IdU followed by CldU 2 h later, and animals survived for 30 min after CldU injection. Antibodies more selective for IdU vs. CldU and vice versa were used to visualize and quantify IdU and CldU cells. Qualitative analysis indicated that IdU cells were labeled with mouse monoclonal BrdU antibody (Fig. 3a–c). CldU cells were labeled with rat monoclonal BrdU antibody (Fig. 3 d–f). BrdU cells were labeled with both mouse and rat monoclonal antibodies to BrdU (not shown). Importantly, the mouse antibody did not label CldU cells, and the rat antibody did not label IdU cells (Fig. 3a, e), demonstrating that the specificity of the labeling can be achieved at the doses tested. Sequential labeling with IdU followed by CldU demonstrated three distinct populations of proliferating cells (Fig. 3 g–i). Cells were only labeled with mouse antibody, only labeled with rat antibody, or labeled with both mouse and rat antibody (Fig. 3i). Quantification of fluorescently labeled IdU, CldU and BrdU in animals injected with one of these markers revealed equivalent numbers of proliferating cells in the SGZ of the hippocampus (IdU: 2329 ± 637 (Abcam); CldU: 2390 ± 540 (Serotec); BrdU (Abcam): 2478 ± 282; BrdU (serotec): 2935 ± 295; $F_{3,7}=0.35$, $p=0.79$).

3.4. Methamphetamine self-administration-induced decreases in S-phase cells and Ki-67 cells is not due to alterations in the duration of the S-phase of the cell cycle

For the calculation of the *S*-phase of the cell cycle, animals from the ShA-13, LgA-13, and drug-naive groups were sequentially injected with IdU followed by CldU 2 h later (see Methods). In animals sequentially injected, IdU^+ cells in the *S*-phase at T = 0 h would have moved into the G_2/M phases of the cell cycle at T = 2 h when CldU was injected (Fig. 3j). At T = 30 min after CldU injection, CldU cells will mostly be in the *S*-phase (Fig. 3j). According to previously published reports, pulse-chasing *S*-phase cells at any given time-point with two *S*-phase markers, such as [^{3}H]thymidine and BrdU (Cameron and McKay, 2001; Hayes and Nowakowski, 2002) or IdU and CldU (Vega and Peterson, 2005), produces three distinct populations of cells. For example, the set of *S*-phase cells labeled at $T_1=0$ h with IdU will be single- (N_{EX}) and double-labeled (N_S) at $T_2=2$ h (Fig. 3j). The set of *S*-phase cells labeled at $T_2=2$ h with CldU will be single- (N_{EN}) and double-labeled (N_S) when euthanized ($T_{CldU}=30$ min; Fig. 3j). All three groups of *S*-phase cells were visible in all of the rats analyzed, with most of the *S*-phase cells double-labeled with CldU and IdU (Fig. 3 k–m and n). The calculation of the *S*-phase length in naive controls revealed a similar timeframe compared with a recent study in adult rats (Olariu et al., 2007) (Fig. 3n, N_S), demonstrating that the BrdU analogs IdU and CldU provide accurate estimates of *S*-phase length compared with BrdU and [^{3}H]thymidine sequential labeling. Methamphetamine significantly reduced the number of cells in N_S but did not alter the number of cells in N_{EN} or N_{EX} ($F_{2,34}=5.15$, $p=0.01$; Fig. 3n, N_S). *Post hoc* analysis indicated that LgA-13 d decreased N_S cells compared with controls ($p=0.01$). Methamphetamine did not alter the duration of the *S*-phase (Fig. 3n, T_S).

3.5. Methamphetamine self-administration distinctly alters the proportion of Ki-67-labeled cells in their preneuronal stages of neuronal development

Hippocampal sections from drug-naive controls and the ShA-4 d, ShA-13 d, LgA-4 d, and LgA-13 d groups were processed and examined for proliferating cell types in discrete stages of neuronal development. Approximately 120 Ki-67-IR cells were analyzed per animal by confocal microscopy to identify and quantify the types of actively dividing neural progenitors through the initial phases of neuronal development (control: 141.7 ± 7.9; ShA-4 d: 125.3 ± 10.1; ShA-13 d: 145.6 ± 11.3; LgA-4 d: 135.1 ± 15.2; LgA-13 d: 108.3 ± 6.7 cells). Scanning was restricted to Ki-67-IR cells that were in the SGZ of the dentate gyrus. Ki-67 cells were colabeled with GFAP, Sox2, and DCX, and co-localization of different markers was used to determine whether a Ki-67 cell was a radial glia-like stem cell ($Ki\text{-}67^+/Sox2^+/GFAP^+$; type1), preneuronal neuroblast ($Ki\text{-}67^+/Sox2^+/DCX^-$; type2a), intermediate cell ($Ki\text{-}67^+/Sox2^+/DCX^+$; type2b), early neuronal cell ($Ki\text{-}67^+/Sox2^-/DCX^+$; type3), or none of these ($Ki\text{-}67^+/GFAP^-/Sox2^-/DCX^-$; Taffe et al., 2010). Methamphetamine altered the ratio of Ki-67 cells that were type1/2a/2b/3 ($F_{4,145}=81.41$, $p<0.0001$). Methamphetamine increased the ratio of $Ki\text{-}67^+/GFAP^+/Sox2^+$ cells ($F_{4,34}=2.7$, $p=0.047$; Fig. 4j), with significant differences between the control and methamphetamine groups. Post hoc analysis revealed significantly higher numbers of $Ki\text{-}67^+/GFAP^+/Sox2^+$ cells in the ShA-13 d group compared with the control, ShA-4 d, and LgA-4 d groups ($p=0.043$, $p=0.055$, and $p=0.034$, respectively; Fig. 4j). Methamphetamine significantly decreased the proportion of $Ki\text{-}67^+/Sox2^+/DCX^-$ cells in all groups ($F_{4,34}=10.491$, $p=0.007$) compared with controls. Post hoc analysis revealed a significantly lower proportion of $Ki\text{-}67^+/Sox2^+/DCX^-$ cells in the ShA-4 d, ShA-13 d, LgA-4 d, and LgA-13 d groups compared with controls ($p's<0.001$ for all groups; Fig. 4j). Methamphetamine did not alter the proportion of $Ki\text{-}67^+/Sox2^+/DCX^+$ cells. Methamphetamine increased the proportion of $Ki\text{-}67^+/Sox2^-/DCX^+$ cells ($F_{4,34}=3.161$, $p=0.016$). Post hoc analysis indicated that ShA-4 d, ShA-13 d, and LgA-4 d animals had a significantly higher number of $Ki\text{-}67^+/Sox2^-/DCX^+$ cells compared with controls ($p's<0.01$ for all groups; Fig. 4j). Methamphetamine did not alter the proportion of Ki-67-only cells in any of the groups.

3.6. Methamphetamine self-administration in LgA-13 d animals decreased the number of immature neurons

Sections from control, ShA-4 d, ShA-13 d, LgA-4 d, and LgA-13 d animals were processed for DCX immunohistochemistry. Sections were stained by DAB reactions, and the total number of DCX^+ cells that were with immature early phase morphology and mature late phase morphology for each group was quantified (Mandyam et al., 2008a, 2008b). The identification of early phase vs. late phase DCX-positive cells was strictly determined based on morphological differences between the two cell types (Fig. 5a). Methamphetamine decreased total (early phase + late phase) DCX + cells ($F_{4,34}=2.105$, $p=0.01$; Fig. 5b). Post hoc analysis indicated a significant decrease in LgA-13 d DCX-IR cells compared with the control ($p=0.038$), ShA-4 d ($p=0.04$), and ShA-13 d ($p=0.029$) groups. The decrease in total DCX-IR cells in LgA-13 d animals was because of decreases in early phase DCX-IR cells ($F_{4,34}=2.184$, $p=0.096$; Fig. 5b). Post hoc analysis indicated that LgA-13 d animals had fewer early phase DCX-IR cells compared with controls ($p=0.008$). Methamphetamine did not alter late phase DCX-IR cells.

3.7. Methamphetamine self-administration in ShA-4 d, ShA-13 d, and LgA-4 d animals increases apoptosis

AC3 was used to label apoptotic cells because it is a marker of apoptosis and a sensitive and reliable method for detecting programmed active cell death (Duan et al., 2003). Most importantly, AC3 labeling is comparable to terminal deoxynucleotidyl transferase (TdT)-mediated dUTP nick-end (TUNEL) labeling (Harburg et al., 2007), another marker used for quantifying apoptotic cells. Sections from control, ShA-4 d, ShA-13 d, LgA-4 d, and LgA-13 d animals were labeled, and DAB-stained AC3 cells were quantified. Methamphetamine

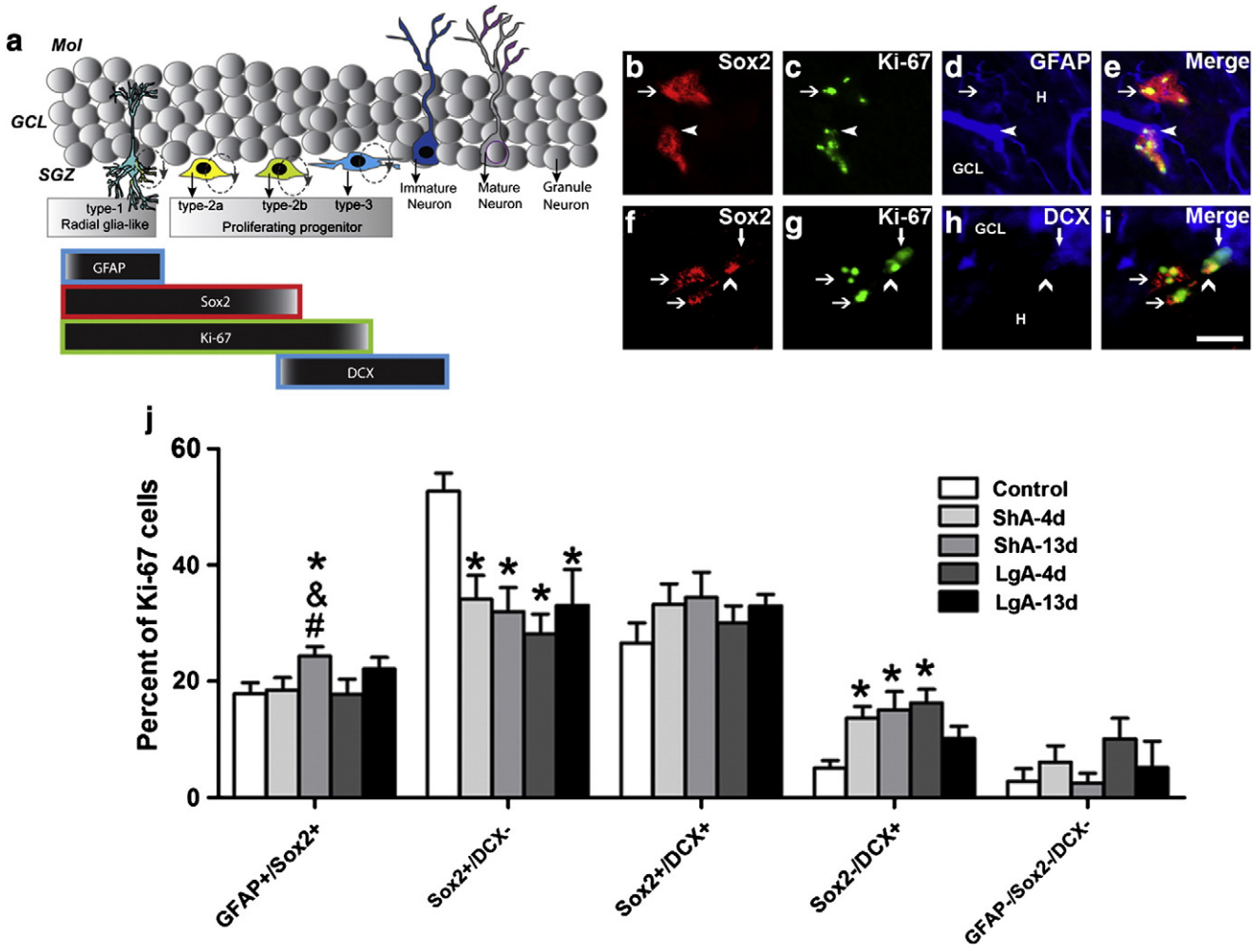

Fig. 4. Methamphetamine self-administration alters the multi-stage process of neuronal development of SGZ progenitors. (a) Schematic of the hippocampal granule cell layer demonstrating the sequence of development of neural progenitors in their initial phases of neuronal development and the markers expressed during the multi-stage process: GFAP, Sox2, Ki-67, and DCX. (b–e) Single *z*-scan (0.5 mm) of a confocal *z*-stack of Sox2-positive cells in red (CY3), Ki-67-positive cells in green (FITC), and GFAP-positive cells in blue (CY5). Arrowheads in (b–e) point to GFAP+/Sox2+/Ki-67+ cells (type1 cells). Thin arrows in (b–e) point to Sox2+/Ki-67+/DCX- cells (type2a cells). (f–i) Single *z*-scan (0.5 mm) of a confocal *z*-stack of Sox2-positive cells in red (CY3), Ki-67-positive cells in green (FITC), and DCX-positive cells in blue (CY5). Arrowheads in (f–i) point to Sox2+/Ki-67+/DCX+ cells (type2b cells). Thick arrows in (f–i) point to Sox2-/Ki-67+/DCX+ cells (type3 cells). Thin arrows in (f–i) point to Sox2+/Ki-67+/DCX- cells (type2a cells). Scale bar in (i) = 10 μm and applies to (f–i). (j) Proportion of Ki-67-IR cells that are type1, 2a, 2b, and 3 and Ki-67-only cells (neither). Data are expressed as mean ± SEM. $^{*}p<0.05$, compared with control; $^{\#}p<0.05$, compared with ShA-4 d; $^{\&}p<0.05$, compared with LgA-4 d.

significantly increased apoptosis ($F_{4,32}=3.476$, $p=0.021$; Fig. 6). *Post hoc* analysis indicated that the ShA-4 d ($p=0.014$), ShA-13 d ($p=0.029$), and LgA-4 d ($p=0.032$) groups had increased AC3 cells compared with controls. AC3 cells in LgA-13 d animals were significantly lower than the other methamphetamine groups ($p<0.05$) and did not significantly differ from control animals.

4. Discussion

The present findings demonstrate the dynamic regulation of hippocampal progenitors by limited vs. extended access methamphetamine and underscore how different durations of methamphetamine access alter distinct aspects of cell cycle dynamics and stages of neuronal development. It is important to note that the observed changes in hippocampal plasticity were measured 14–22 h after the last methamphetamine intake. Given that the elimination rate of i.v. methamphetamine measured by $t_{1/2}$ values in adult rats is approximately an hour (Riviere et al., 1999), the alterations in SGZ progenitor cell cycle dynamics and development could be attributable to the chronic administration paradigm of methamphetamine, and not to immediate effects of the drug. The results, therefore, suggest that certain neuromodulatory effects in the brain are perhaps more sensitive to the amount of daily methamphetamine intake and confirm that higher amounts of methamphetamine intake produce more pronounced effects on neuroplastic events that are affected by addiction.

Methamphetamine self-administration (LgA-4 d and LgA-13 d) decreased proliferating Ki-67 cells, supporting and confirming a previous report (Mandyam et al., 2008b). Therefore, alterations in cell cycle dynamics of proliferating cells that could be responsible for methamphetamine-induced inhibition of proliferation were analyzed. The analysis of CldU cells demonstrated that the decrease in Ki-67 cells was due to a reduced number of cells in the *S*-phase of the cell cycle (LgA-4 d and LgA-13 d), reflected by decreased CldU cells. As reported by several studies, Ki-67 and CldU label different aspects of the cell cycle. Ki-67 is expressed in cells during all phases of the cell cycle (*S*, G_2, *M*, and G_1; Scholzen and Gerdes, 2000), whereas CldU is only incorporated into the cells during the *S*-phase of the cell cycle (Eisch and Mandyam, 2004). Therefore, reduced Ki-67 cells and CldU cells in LgA-4 d and LgA-13 d animals suggests that the decreased progenitor pool is due to fewer cells in the *S*-phase. However, reduced CldU cells and a normal number of Ki-67 cells in the ShA-13 d group suggest that proliferating cells are probably arrested in the G_1 phase of

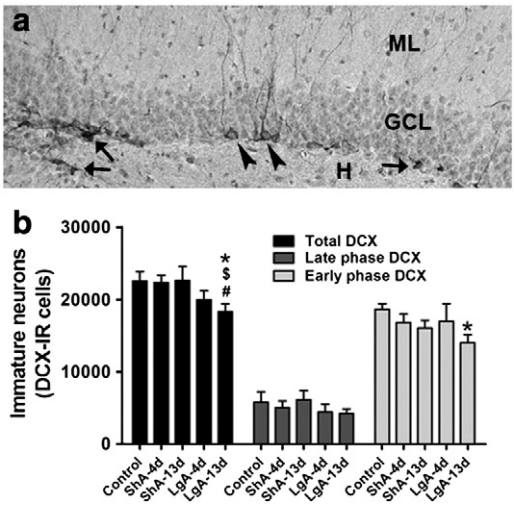

Fig. 5. Methamphetamine self-administration decreases the number of DCX cells. (a) Photomicrograph of DCX staining in the dentate gyrus of a control animal. Arrowheads in (a) point to a mature DCX cell, and arrows in (a) point to immature DCX cells. GCL, granule cell layer; ML, molecular layer; H, hilus. (b) Total number of DCX-IR cells in control, ShA-4 d, ShA-13 d, LgA-4 d, and LgA-13 d were quantified. DCX-IR cells were also separated, based on morphology, into early-phase and late-phase DCX-positive cells. Black bars, total number of DCX-IR cells; gray bars, total number of late-phase DCX-IR cells; white bars, total number of early-phase DCX-IR cells. $^{*}p<0.05$, compared with control; $^{\$}p<0.05$, compared with ShA-13 d; $^{\#}p<0.05$, compared with ShA-4 d.

the cell cycle (Morris et al., 2009). The comparison of Ki-67 and CldU data suggests that methamphetamine-induced inhibition of proliferation is probably due to a shortened *S*-phase or reduced pool of neural progenitors that could be produced by arresting cells in the G_1 phase, followed by killing cells in the G_1 phase or G_1/S checkpoint of the cell cycle.

Sequential administration of the BrdU analogs IdU and CldU was performed to determine the length of the *S*-phase of hippocampal progenitors and examine whether changes in *S*-phase dynamics contributed to the decreased *S*-phase cells and Ki-67 cells. Key technical elements for the *S*-phase analysis were first examined. The specificity of the two antibodies (mouse monoclonal anti-BrdU to label only IdU and rat monoclonal anti-BrdU to label only CldU) for distinguishing IdU vs. CldU have been tested for equi-molar doses of the markers at saturating and lower non-saturating doses in adult rats (Leuner et al., 2009; Thomas et al., 2007; Vega and Peterson, 2005). The specificity of the antibodies for IdU and CldU is optimal at lower doses of the markers (Thomas et al., 2007; Vega and Peterson, 2005) and disappears at higher saturating doses (Leuner et al., 2009). From these studies, it appears that the *S*-phase analysis with IdU and CldU is accompanied by a potential caveat such as a trade-off between saturation and specificity of the two analogs, and it may not be possible to achieve both.

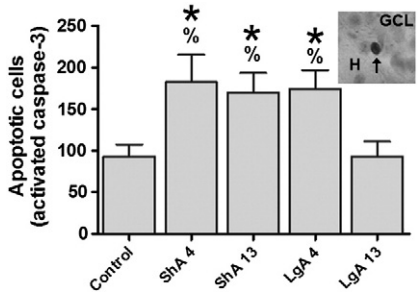

Fig. 6. Methamphetamine self-administration increases apoptosis. Quantitative analysis of the total number of apoptotic cells (AC3-IR cells) in control, ShA-4 d, ShA-13 d, LgA-4 d, and LgA-13 d. $^{*}p<0.05$, compared with control; $^{\%}p<0.05$, compared with LgA-13 d. Inset shows a positively stained AC3-IR cell in the SGZ of the DG. GCL, granule cell layer; H, hilus.

However, labeling the same subpopulation of *S*-phase cells with equi-effective doses of BrdU analogs should provide correct estimates of S-phase length. This is based on the assumption that labeling identical, albeit incomplete, *S*-phase subpopulation by multiple BrdU analogs should not affect the mathematical analysis. Therefore, equi-effective doses of IdU and CldU were injected, and antibodies that were selective for labeling each of the markers were used to determine the length of the *S*-phase of hippocampal neural progenitors. The results demonstrate that the doses of IdU and CldU used in our study label equal numbers of hippocampal progenitors in the *S*-phase compared with the gold standard marker BrdU, and presumably the same subpopulation of *S*-phase cells. The results also show that the length of the *S*-phase estimate in drug-naive animals using IdU and CldU does not significantly differ from a previous study that estimated the length of the *S*-phase with BrdU and [^{3}H]thymidine (Olariu et al., 2007; Fig. 3f, T_S). The current findings also show that methamphetamine self-administration does not alter the length of the *S*-phase, indicating that reduced S-phase cells by methamphetamine is not due to altered *S*-phase dynamics of proliferating progenitors. The lack of effect on *S*-phase length by methamphetamine by double *S*-phase labeling with IdU/CldU is further supported by co-labeling analysis of Ki-67 and CldU, where the proportion of Ki-67 cells in the *S*-phase (CldU) remains unchanged in all of the methamphetamine groups. Unchanged *S*-phase dynamics by methamphetamine was not surprising because insults such as chemicals, radiation, faulty replication, and drugs, including morphine and caffeine, alter other phases of the cell cycle, such as the G_2/M checkpoint or G_2/M phase (Arguello et al., 2008; Chappell and Dalton, 2010; Mandyam et al., 2004; Schlegel et al., 1987). Therefore, these results support the speculation that the duration of the *S*-phase of the cell cycle is most preserved and least sensitive to modifications (Eisch and Mandyam, 2007; Ford and Pardee, 1998; Katou et al., 2003).

In addition to exploring the effects of methamphetamine self-administration on the cell cycle dynamics of proliferating cells, the effects of methamphetamine on the development of Ki-67 cells were investigated. Ki-67 is expressed in a heterogeneous population of proliferating progenitor cells in the SGZ, and Ki-67 labeling can be used to identify distinct neural developmental stages (namely type1/2a/2b/3) of proliferating progenitors (Filippov et al., 2003; Kronenberg et al., 2003; Steiner et al., 2006; Taffe et al., 2010). Using the combination of Ki-67 and DCX, it has been previously demonstrated that prolonged methamphetamine self-administration (ShA-42 d and LgA-42 d) inhibits hippocampal neurogenesis by decreasing the number of intermediate/early neuronal type2b/3 cell types (Mandyam et al., 2008b). In the present study, methamphetamine-induced inhibition or activation of earlier cell types (such as type1 and type2a) was assessed to determine a mechanism for methamphetamine-induced inhibition of proliferation. We hypothesized that methamphetamine self-administration-induced inhibition of Ki-67 cells that were either radial glia-like stem cells or preneuronal neuroblasts (precursors of the later immature neuronal type2b/3 cell types; (Steiner et al., 2006)) would contribute to the altered development of proliferating cells. Methamphetamine (ShA-13 d) increased the proportion of proliferating type1 radial glia-like stem cells ($GFAP^+/Sox2^+/Ki\text{-}67^+$) and decreased the proportion of proliferating type2a preneuronal neuroblasts ($Sox2^+/Ki\text{-}67^+/DCX^-$). This very interesting finding adds to the growing literature showing that the preneuronal stages of a proliferating cell influences its response to stimuli (Arguello et al., 2008; Tashiro et al., 2007). The comparison of Ki-67, CldU, and Ki-67/Sox2 data in ShA-4 d animals suggests that the reduced proportion of proliferating type2a cells could be due to the altered expression of Sox2 protein by methamphetamine and that methamphetamine-induced alteration of intrinsic proteins could partially contribute to reduced proliferation.

Methamphetamine enhanced the proportion of proliferating type3 preneuronal progenitors ($Sox2^-/Ki\text{-}67^+/DCX^+$) in ShA-4 d, ShA-13 d, and LgA-4 d animals. Additional analysis in ShA-4 d, ShA-13 d, and LgA-4 d animals demonstrated normal levels of DCX cells, indicating that the enhanced proportion of $Sox2^-/Ki\text{-}67^+/DCX^+$ cells in these animals did not result from an altered number of DCX cells. This finding suggests that only a subpopulation of DCX cells is sensitive to methamphetamine during earlier sessions of self-administration. In LgA-13 d animals, methamphetamine did not produce an alteration in $Sox2^-/Ki\text{-}67^+/DCX^+$ cell type but decreased the number of DCX cells (particularly the early phase DCX cells). This interesting finding could be attributable to a reduced pool of cycling preneuronal progenitors or the timeframe and amount of methamphetamine exposure in the LgA-13 d group because the regulation of DCX expression could require a longer timeframe compared with proliferation (Brown et al., 2003). Given that the plasticity and functioning of immature neurons is regulated by the maturation and integration of immature neurons into the hippocampal circuitry (Doetsch and Hen, 2005), these results suggest that the disruption of maturation of DCX cells by methamphetamine may contribute to maladaptive plasticity in the hippocampus. Future work could address this hypothesis by evaluating whether the dendritic morphology of DCX cells is altered after methamphetamine exposure, which has been assessed after antidepressant administration, seizures, or drug of abuse administration (Hernandez-Rabaza et al., 2006; Jessberger et al., 2005; Wang et al., 2008).

Another important finding from the present work is that methamphetamine increased apoptotic cell death in the SGZ very early during the self-administration paradigm (ShA-4 d). The enhanced cell death appears to be maintained in the limited access paradigm over a prolonged timeframe. ShA-13 d animals from this study and ShA-42 d animals from a previous study (Mandyam et al., 2008b) continued to show increased apoptotic cells. In the extended access paradigm, cell death was evident early during the self-administration paradigm (LgA-4 d) and did not occur in LgA-13 d or LgA-42 d animals (Mandyam et al., 2008b). Cell death in ShA-4 d, ShA-13 d, and LgA-4 d animals could reflect dying progenitors whose loss could result in decreased proliferation or dying post-mitotic neurons whose loss could result in decreased survival. Therefore, decreased *S*-phase cells in ShA-13 d and LgA-4 d animals could be due to cell death. However, decreased *S*-phase cells in LgA-13 d animals could reflect a new homeostatic number of proliferating cells. Technically challenging experiments, including phenotyping apoptotic cells (Bauer and Patterson, 2005; Cooper-Kuhn and Kuhn, 2002), could support this hypothesis. The results, therefore, suggest that methamphetamine-induced regulation of hippocampal apoptosis is perhaps more sensitive to the amount of daily methamphetamine intake and confirm that higher amounts of methamphetamine intake in LgA-13 d animals regulate methamphetamine excitotoxicity by other forms of cell death including necrosis and neurodegeneration (Yamamoto et al., 2010).

In summary, our results demonstrate that LgA methamphetamine-induced inhibition of hippocampal proliferation results from a decreased pool of *S*-phase progenitors without specific alterations in the dynamics of the *S*-phase of the cell cycle. LgA methamphetamine-induced inhibition of immature neurons results from maladaptive modifications in the development of neural progenitors and increases in cell death. The functional implication of these findings, albeit speculative, is important to consider because they may influence our understanding of methamphetamine addiction. For example, given that the hippocampus is tactically situated in the brain to communicate with the other brain reward regions, such as the prefrontal cortex and amygdala, to play a significant role in drug context-specific memories associated with drug taking and relapse to drug seeking (Black et al., 2004; Lansink et al., 2009; Ricoy and Martinez, 2009), it can be hypothesized that alterations in the birth and plasticity of hippocampal granule neurons by methamphetamine could be involved in the neuroplasticity of methamphetamine addiction. Our findings, therefore, establish hippocampal neurogenesis as a potential target for therapeutic approaches to treat methamphetamine addiction.

Acknowledgements

The study was supported by funds from the National Institute on Drug Abuse (DA022473 to CDM) and Skaggs School of Pharmacy and Pharmaceutical Sciences (Skaggs Scholarship to CJY). We acknowledge the excellent technical assistance of Roxanne Kotzebue and Matthew Soleiman from the independent study program at the University of California, San Diego, and Patrick Recinto from the College of Pharmacy at the University of California, San Diego, for assistance with immunohistochemistry. We thank Dr. Giridhar Mandyam for assistance with mathematical calculations for the *S*-phase study and Dr. Scott Edwards for assistance with the statistical analyses. We appreciate the technical support of Elena Crawford and Robert Lintz and the editorial assistance of Michael Arends. The authors report no biomedical financial interests or potential conflicts of interest. This is publication number 21011 from The Scripps Research Institute.

References

Altman J, Das GD. Autoradiographic and histological evidence of postnatal hippocampal neurogenesis in rats. J Comp Neurol 1965;124:319–35.
Arguello AA, Harburg GC, Schonborn JR, Mandyam CD, Yamaguchi M, Eisch AJ. Time course of morphine's effects on adult hippocampal subgranular zone reveals preferential inhibition of cells in S phase of the cell cycle and a subpopulation of immature neurons. Neuroscience 2008;157:70–9.
Bauer S, Patterson PH. The cell cycle-apoptosis connection revisited in the adult brain. J Cell Biol 2005;171:641–50.
Black YD, Green-Jordan K, Eichenbaum HB, Kantak KM. Hippocampal memory system function and the regulation of cocaine self-administration behavior in rats. Behav Brain Res 2004;151:225–38.
Breunig JJ, Silbereis J, Vaccarino FM, Sestan N, Rakic P. Notch regulates cell fate and dendrite morphology of newborn neurons in the postnatal dentate gyrus. Proc Natl Acad Sci USA 2007;104:20558–63.
Brown JP, Couillard-Despres S, Cooper-Kuhn CM, Winkler J, Aigner L, Kuhn HG. Transient expression of doublecortin during adult neurogenesis. J Comp Neurol 2003;467:1–10.
Brown TE, Lee BR, Ryu V, Herzog T, Czaja K, Dong Y. Reducing hippocampal cell proliferation in the adult rat does not prevent the acquisition of cocaine-induced conditioned place preference. Neurosci Lett 2010;481:41–6.
Burns KA, Kuan CY. Low doses of bromo- and iododeoxyuridine produce near-saturation labeling of adult proliferative populations in the dentate gyrus. Eur J Neurosci 2005;21:803–7.
Cameron HA, McKay RD. Adult neurogenesis produces a large pool of new granule cells in the dentate gyrus. J Comp Neurol 2001;435:406–17.
Canales JJ. Adult neurogenesis and the memories of drug addiction. Eur Arch Psychiatry Clin Neurosci 2007;257:261–70.
Canales JJ. Comparative neuroscience of stimulant-induced memory dysfunction: role for neurogenesis in the adult hippocampus. Behav Pharmacol 2010;21:379–93.
Chappell J, Dalton S. Altered cell cycle regulation helps stem-like carcinoma cells resist apoptosis. BMC Biol 2010;8:63.
Cooper-Kuhn CM, Kuhn HG. Is it all DNA repair? Methodological considerations for detecting neurogenesis in the adult brain. Brain Res Dev Brain Res 2002;134:13–21.
Cosgrove KP, Hunter RG, Carroll ME. Wheel-running attenuates intravenous cocaine self-administration in rats: sex differences. Pharmacol Biochem Behav 2002;73:663–71.
Doetsch F, Hen R. Young and excitable: the function of new neurons in the adult mammalian brain. Curr Opin Neurobiol 2005;15:121–8.
Duan WR, Garner DS, Williams SD, Funckes-Shippy CL, Spath IS, Blomme EA. Comparison of immunohistochemistry for activated caspase-3 and cleaved cytokeratin 18 with the TUNEL method for quantification of apoptosis in histological sections of PC-3 subcutaneous xenografts. J Pathol 2003;199:221–8.
Earnheart JC, Schweizer C, Crestani F, Iwasato T, Itohara S, Mohler H, et al. GABAergic control of adult hippocampal neurogenesis in relation to behavior indicative of trait anxiety and depression states. J Neurosci 2007;27:3845–54.
Eisch AJ, Harburg GC. Opiates, psychostimulants, and adult hippocampal neurogenesis: Insights for addiction and stem cell biology. Hippocampus 2006;16:271–86.
Eisch AJ, Mandyam CD. Beyond BrdU: Basic and clinical implications for analysis of endogenous cell cycle proteins. Progress in stem cell research. Nova Science Publishers Inc; 2004.
Eisch AJ, Mandyam CD. Adult neurogenesis: can analysis of cell cycle proteins move us "Beyond BrdU"? Curr Pharm Biotechnol 2007;8:147–65.
Encinas JM, Vaahtokari A, Enikolopov G. Fluoxetine targets early progenitor cells in the adult brain. Proc Natl Acad Sci USA 2006;103:8233–8.

Filippov V, Kronenberg G, Pivneva T, Reuter K, Steiner B, Wang LP, et al. Subpopulation of nestin-expressing progenitor cells in the adult murine hippocampus shows electrophysiological and morphological characteristics of astrocytes. Mol Cell Neurosci 2003;23:373–82.
Ford HL, Pardee AB. The S phase: beginning, middle, and end: a perspective. J Cell Biochem Suppl 1998;30–31:1–7.
Ge S, Yang CH, Hsu KS, Ming GL, Song H. A critical period for enhanced synaptic plasticity in newly generated neurons of the adult brain. Neuron 2007;54:559–66.
Gerdes J, Lemke H, Baisch H, Wacker HH, Schwab U, Stein H. Cell cycle analysis of a cell proliferation-associated human nuclear antigen defined by the monoclonal antibody Ki-67. J Immunol 1984;133:1710–5.
Gould E, Beylin A, Tanapat P, Reeves A, Shors TJ. Learning enhances adult neurogenesis in the hippocampal formation. Nat Neurosci 1999;2:260–5.
Harburg GC, Hall FS, Harrist AV, Sora I, Uhl GR, Eisch AJ. Knockout of the mu opioid receptor enhances the survival of adult-generated hippocampal granule cell neurons. Neuroscience 2007;144:77–87.
Hastings NB, Tanapat P, Gould E. Neurogenesis in the adult mammalian brain. Clin Neurosci Res 2001;1:175–82.
Hayes NL, Nowakowski RS. Exploiting the dynamics of S-phase tracers in developing brain: interkinetic nuclear migration for cells entering versus leaving the S-phase. Dev Neurosci 2000;22:44–55.
Hayes NL, Nowakowski RS. Dynamics of cell proliferation in the adult dentate gyrus of two inbred strains of mice. Brain Res Dev Brain Res 2002;134:77–85.
Hernandez-Rabaza V, Dominguez-Escriba L, Barcia JA, Rosel JF, Romero FJ, Garcia-Verdugo JM, et al. Binge administration of 3,4-methylenedioxymethamphetamine ("ecstasy") impairs the survival of neural precursors in adult rat dentate gyrus. Neuropharmacology 2006;51:967–73.
Hildebrandt K, Teuchert-Noodt G, Dawirs RR. A single neonatal dose of methamphetamine suppresses dentate granule cell proliferation in adult gerbils which is restored to control values by acute doses of haloperidol. J Neural Transm 1999;106:549–58.
Jessberger S, Romer B, Babu H, Kempermann G. Seizures induce proliferation and dispersion of doublecortin-positive hippocampal progenitor cells. Exp Neurol 2005;196:342–51.
Kaplan MS, Hinds JW. Neurogenesis in the adult rat: electron microscopic analysis of light radioautographs. Science 1977;197:1092–4.
Katou Y, Kanoh Y, Bando M, Noguchi H, Tanaka H, Ashikari T, et al. S-phase checkpoint proteins Tof1 and Mrc1 form a stable replication-pausing complex. Nature 2003;424:1078–83.
Kitamura O, Wee S, Specio SE, Koob GF, Pulvirenti L. Escalation of methamphetamine self-administration in rats: a dose-effect function. Psychopharmacology (Berl) 2006;186:48–53.
Kochman LJ, Fornal CA, Jacobs BL. Suppression of hippocampal cell proliferation by short-term stimulant drug administration in adult rats. Eur J Neurosci 2009;29:2157–65.
Kronenberg G, Reuter K, Steiner B, Brandt MD, Jessberger S, Yamaguchi M, et al. Subpopulations of proliferating cells of the adult hippocampus respond differently to physiologic neurogenic stimuli. J Comp Neurol 2003;467:455–63.
Lansink CS, Goltstein PM, Lankelma JV, McNaughton BL, Pennartz CM. Hippocampus leads ventral striatum in replay of place-reward information. PLoS Biol 2009;7:e1000173.
Leuner B, Glasper ER, Gould E. Thymidine analog methods for studies of adult neurogenesis are not equally sensitive. J Comp Neurol 2009;517:123–33.
Madsen TM, Kristjansen PE, Bolwig TG, Wortwein G. Arrested neuronal proliferation and impaired hippocampal function following fractionated brain irradiation in the adult rat. Neuroscience 2003;119:635–42.
Mandyam CD, Crawford EF, Eisch AJ, Rivier CL, Richardson HN. Stress experienced in utero reduces sexual dichotomies in neurogenesis, microenvironment, and cell death in the adult rat hippocampus. Dev Neurobiol 2008a;68:575–89.
Mandyam CD, Norris RD, Eisch AJ. Chronic morphine induces premature mitosis of proliferating cells in the adult mouse subgranular zone. J Neurosci Res 2004;76:783–94.
Mandyam CD, Wee S, Crawford EF, Eisch AJ, Richardson HN, Koob GF. Varied access to intravenous methamphetamine self-administration differentially alters adult hippocampal neurogenesis. Biol Psychiatry 2008b;64:958–65.
Mandyam CD, Wee S, Eisch AJ, Richardson HN, Koob GF. Methamphetamine self-administration and voluntary exercise have opposing effects on medial prefrontal cortex gliogenesis. J Neurosci 2007;27:11442–50.
Maslov AY, Barone TA, Plunkett RJ, Pruitt SC. Neural stem cell detection, characterization, and age-related changes in the subventricular zone of mice. J Neurosci 2004;24:1726–33.
Morgan ME, Gibb JW. Short-term and long-term effects of methamphetamine on biogenic amine metabolism in extra-striatal dopaminergic nuclei. Neuropharmacology 1980;19:989–95.
Morris SA, Eaves DW, Smith AR, Nixon K. Alcohol inhibition of neurogenesis: a mechanism of hippocampal neurodegeneration in an adolescent alcohol abuse model. Hippocampus 2010;20(5):596–607.
Newton TF, De La Garza 2nd R, Kalechstein AD, Tziortzis D, Jacobsen CA. Theories of addiction: methamphetamine users' explanations for continuing drug use and relapse. Am J Addict 2009;18:294–300.
Noonan MA, Bulin SE, Fuller DC, Eisch AJ. Reduction of adult hippocampal neurogenesis confers vulnerability in an animal model of cocaine addiction. J Neurosci 2010;30:304–15.
Noonan MA, Choi KH, Self DW, Eisch AJ. Withdrawal from cocaine self-administration normalizes deficits in proliferation and enhances maturity of adult-generated hippocampal neurons. J Neurosci 2008;28:2516–26.
Nowakowski RS, Lewin SB, Miller MW. Bromodeoxyuridine immunohistochemical determination of the lengths of the cell cycle and the DNA-synthetic phase for an anatomically defined population. J Neurocytol 1989;18:311–8.
Olariu A, Cleaver KM, Cameron HA. Decreased neurogenesis in aged rats results from loss of granule cell precursors without lengthening of the cell cycle. J Comp Neurol 2007;501:659–67.
Paxinos G, Watson C. The rat brain in stereotaxic coordinates. 3 rd ed. San Diego: Academic Press; 1997.
Raber J, Rola R, LeFevour A, Morhardt D, Curley J, Mizumatsu S, et al. Radiation-induced cognitive impairments are associated with changes in indicators of hippocampal neurogenesis. Radiat Res 2004;162:39–47.
Ricoy UM, Martinez Jr JL. Local hippocampal methamphetamine-induced reinforcement. Front Behav Neurosci 2009;3:47.
Riviere GJ, Byrnes KA, Gentry WB, Owens SM. Spontaneous locomotor activity and pharmacokinetics of intravenous methamphetamine and its metabolite amphetamine in the rat. J Pharmacol Exp Ther 1999;291:1220–6.
Roehr B. Half a million Americans use methamphetamine every week. BMJ 2005;331:476.
Rogers JL, De Santis S, See RE. Extended methamphetamine self-administration enhances reinstatement of drug seeking and impairs novel object recognition in rats. Psychopharmacology (Berl) 2008;199:615–24.
Rola R, Raber J, Rizk A, Otsuka S, VandenBerg SR, Morhardt DR, et al. Radiation-induced impairment of hippocampal neurogenesis is associated with cognitive deficits in young mice. Exp Neurol 2004;188:316–30.
Schlegel R, Croy RG, Pardee AB. Exposure to caffeine and suppression of DNA replication combine to stabilize the proteins and RNA required for premature mitotic events. J Cell Physiol 1987;131:85–91.
Schmued LC, Bowyer JF. Methamphetamine exposure can produce neuronal degeneration in mouse hippocampal remnants. Brain Res 1997;759:135–40.
Scholzen T, Gerdes J. The Ki-67 protein: from the known and the unknown. J Cell Physiol 2000;182:311–22.
Schwartz DL, Mitchell AD, Lahna DL, Luber HS, Huckans MS, Mitchell SH, et al. Global and local morphometric differences in recently abstinent methamphetamine-dependent individuals. Neuroimage 2010;50:1392–401.
Shors TJ, Townsend DA, Zhao M, Kozorovitskiy Y, Gould E. Neurogenesis may relate to some but not all types of hippocampal-dependent learning. Hippocampus 2002;12:578–84.
Simon SL, Dean AC, Cordova X, Monterosso JR, London ED. Methamphetamine dependence and neuropsychological functioning: evaluating change during early abstinence. J Stud Alcohol Drugs 2010;71:335–44.
Smith MA, Schmidt KT, Iordanou JC, Mustroph ML. Aerobic exercise decreases the positive-reinforcing effects of cocaine. Drug Alcohol Depend 2008;98:129–35.
Smith MA, Walker KL, Cole KT, Lang KC. The effects of aerobic exercise on cocaine self-administration in male and female rats. Psychopharmacology (Berl) 2011.
Steiner B, Klempin F, Wang L, Kott M, Kettenmann H, Kempermann G. Type-2 cells as link between glial and neuronal lineage in adult hippocampal neurogenesis. Glia 2006;54:805–14.
Sudai E, Croitoru O, Shaldubina A, Abraham L, Gispan I, Flaumenhaft Y, et al. High cocaine dosage decreases neurogenesis in the hippocampus and impairs working memory. Addict Biol 2011;16:251–60.
Taffe MA, Kotzebue RW, Crean RD, Crawford EF, Edwards S, Mandyam CD. Long-lasting reduction in hippocampal neurogenesis by alcohol consumption in adolescent nonhuman primates. Proc Natl Acad Sci USA 2010;107:11104–9.
Tashiro A, Makino H, Gage FH. Experience-specific functional modification of the dentate gyrus through adult neurogenesis: a critical period during an immature stage. J Neurosci 2007;27:3252–9.
Teuchert-Noodt G, Dawirs RR, Hildebrandt K. Adult treatment with methamphetamine transiently decreases dentate granule cell proliferation in the gerbil hippocampus. J Neural Transm 2000;107:133–43.
Thanos PK, Tucci A, Stamos J, Robison L, Wang GJ, Anderson BJ, et al. Chronic forced exercise during adolescence decreases cocaine conditioned place preference in Lewis rats. Behav Brain Res 2010;215:77–82.
Thomas RM, Hotsenpiller G, Peterson DA. Acute psychosocial stress reduces cell survival in adult hippocampal neurogenesis without altering proliferation. J Neurosci 2007;27:2734–43.
Thompson PM, Hayashi KM, Simon SL, Geaga JA, Hong MS, Sui Y, et al. Structural abnormalities in the brains of human subjects who use methamphetamine. J Neurosci 2004;24:6028–36.
UNODC. World drug report. Vienna, Austria: United Nations Office on Drugs and Crime; 2009 http://wwwunodcorg/documents/wdr/WDR_2009/webpdf.
van Praag H, Christie BR, Sejnowski TJ, Gage FH. Running enhances neurogenesis, learning, and long-term potentiation in mice. Proc Natl Acad Sci USA 1999a;96:13427–31.
van Praag H, Kempermann G, Gage FH. Running increases cell proliferation and neurogenesis in the adult mouse dentate gyrus. Nat Neurosci 1999b;2:266–70.
Vega CJ, Peterson DA. Stem cell proliferative history in tissue revealed by temporal halogenated thymidine analog discrimination. Nat Methods 2005;2:167–9.
Wang JW, David DJ, Monckton JE, Battaglia F, Hen R. Chronic fluoxetine stimulates maturation and synaptic plasticity of adult-born hippocampal granule cells. J Neurosci 2008;28:1374–84.
Yamamoto BK, Moszczynska A, Gudelsky GA. Amphetamine toxicities: classical and emerging mechanisms. Ann N Y Acad Sci 2010;1187:101–21.